

1 **SWMManywhere: A Global-scale Workflow for** 2 **Generation and Sensitivity Analysis of Synthetic** 3 **Urban Drainage Models**

4 Barnaby Dobson¹, Tijana Jovanovic², Diego Alonso-Álvarez³, Taher Chegini⁴

5 ¹Department of Civil Engineering, Imperial College London, UK

6 ²British Geological Survey, UK

7 ³Research Computing Service, Information and Communication Technologies (RCS-ICT),
8 Imperial College London, UK

9 ⁴Purdue University, USA

10 11 **Statement**

12 The submitted version on EarthArXiv is a non-peer reviewed preprint. This manuscript has,
13 however, been submitted for peer review in the Environmental Modelling and Software.

14 Subsequent versions of this manuscript may have slightly different content. If accepted, the
15 final version of this manuscript will be available via the 'Peer-reviewed Publication DOI' link
16 on the right-hand side of this webpage.

17 **Highlights**

- 18 - SWMMAnywhere can synthesise an urban drainage network model anywhere in the
19 world
- 20 - SWMMAnywhere is a parameterised approach for customising the synthesised
21 network
- 22 - We use sensitivity analysis to investigate uncertainty of network synthesis
- 23 - We find significant interaction between parameters, suggesting an ensemble
24 approach
- 25 - Parameters controlling surface observable network elements are most sensitive

26 **Abstract**

27 Continual improvements in publicly available global geospatial datasets provide an
28 opportunity for deriving urban drainage networks and simulation models of these networks
29 (UDMs) worldwide. We present SWMMAnywhere, which leverages such datasets for
30 generating synthetic UDMs and creating a Storm Water Management Model for any urban
31 area globally. SWMMAnywhere's highly modular and parameterised approach enables
32 significant customisation to explore hydraulically feasible network configurations. Key novelties
33 of our workflow are in network topology derivation that accounts for combined effects of
34 impervious area and pipe slope. We assess SWMMAnywhere by comparing pluvial flooding,
35 drainage network outflows, and design with known networks. The results demonstrate high
36 quality simulations are achievable with a synthetic approach even for large networks. Our
37 extensive sensitivity analysis shows that the locations of manholes, outfalls, and underlying
38 street network are the most sensitive parameters. We find widespread sensitivity across all
39 parameters without clearly defined values that they should take, thus, recommending an
40 uncertainty driven approach to synthetic drainage network modelling. This study showcases
41 significant potential of SWMMAnywhere for research and industry applications to provide
42 drainage network models in urban areas where traditional approaches are impractical.

43 **1 Introduction**

44 Urban drainage models (UDMs) are representations of land and pipes that can be simulated
45 with hydraulic models such as Storm Water Management Model (SWMM) (Rossman, 2010).
46 UDMs are essential for managing stormwater, preventing flooding, and ensuring the
47 sustainability of urban water systems (Butler and Davies, 2004). UDM simulations capture
48 the behaviour of drainage networks under various rainfall scenarios, enabling planners to
49 design effective infrastructure and mitigate risks (Bach et al., 2014). However, the
50 development of UDMs typically requires extensive infrastructure records on the connectivity,
51 geometric properties, and elevations of underground pipes (Bach et al., 2020; Chahinian et
52 al., 2019). In cases where these records are unavailable, whether due to ownership issues
53 or simply that they do not exist, the expense of creating a UDM becomes significant because
54 of costly surveying requirements. To forgo this expense, it may be preferable to synthesise
55 a UDM based on the underlying information governing the placement and sizing of drainage
56 pipes, most generally, surface elevation, building locations, and road locations (Chegini and
57 Li, 2022).

58 The earliest methods to create synthetic UDM exploited the fractal nature of a drainage
59 network and, while simulations were not tested, demonstrated that the broad statistical
60 properties of the network, i.e., distribution of flow path lengths, could be estimated (Ghosh et
61 al., 2006). When road network and elevation data were incorporated, the accuracy of
62 synthesised UDMs improved and simulations approached those of a real UDM for the same
63 locale (Blumensaat et al., 2012). Generally, UDM synthesis involves three main tasks:
64 delineating surface characteristics, deriving network topology, and hydraulic design, each of
65 which will be reviewed below.

66 First, surface characteristics, hereafter referred to as sub-catchments, quantify the spatial
67 distribution of stormwater drainage from impervious areas to manholes. Sub-catchment
68 delineation has received the least attention in UDM synthesis literature and most commonly
69 follows a watershed delineation approach (Blumensaat et al., 2012; Warsta et al., 2017). The

70 drained impervious area within a delineated sub-catchment is typically calculated from the
71 area covered by roads and buildings (Mair et al., 2017; Chegini and Li, 2022). However,
72 another simpler method is to assign impervious areas to drain to a nearest manhole (Reyes-
73 Silva et al., 2023). Both methods require identification of manholes, highlighted as critical
74 future work in Blumensaat et al., (2012), but has received little attention since (Bertsch et al.,
75 2017; Chahinian et al., 2019). We place sub-catchment delineation and manhole
76 identification as the first tasks to perform during UDM synthesis, since network topology and
77 hydraulic design should account for the impervious area contributing to a given pipe.

78 Second, network topology describes the spatial layout of a UDM, connectivity of pipes, and
79 connectivity of the sub-catchments to UDM, i.e., through manholes. Network topology is
80 typically derived by asserting that pipes follow roads, thus dramatically reducing the
81 dimensionality of deriving network topology (Mair et al., 2017; Xu et al., 2021). An efficient
82 network that visits all manholes without redundant pipes can be derived using a shortest
83 path-based algorithm. This algorithm minimizes the total graph cost, with each edge (i.e., a
84 plausible pipe) assigned an individual cost that represents some penalty associated with
85 retaining that edge. Chahinian et al. (2019) provide a detailed exploration minimising costs
86 based on pipe length, pipe adjacent angle, and slope, and highlighting the importance of
87 slope as a cost. Reyes-Silva et al. (2023) derive the UDM by applying the minimum
88 spanning tree (MST) to a full street network to minimise the number of pipes. This approach,
89 however, does not inherently consider slope in the deriving network topology step since MST
90 is only applicable to undirected networks, instead gravitational slope along pipes is enforced
91 as a postprocessing correction. A minimum spanning arborescence is an alternative
92 approach to solve such a problem for a directed network (Ray and Sen, 2024; Tarjan, 1977),
93 although has not yet been demonstrated in UDM synthesis. Furthermore, an additional cost
94 to be minimised that has not been tested in the literature is the need to minimise the
95 impervious contributing area to a given pipe and thus more evenly distribute flow throughout

96 the network, much in the manner of the original proposed fractals for network topology
97 (Ghosh et al., 2006).

98 Third, hydraulic design refers to the selection of pipe diameter, invert levels, and other pipe
99 hydraulic parameters in a synthetic UDM, which typically follows local standards (Chegini
100 and Li, 2022; Duque et al., 2022; Reyes-Silva et al., 2023). Duque et al. (2022), present a
101 methodology for designing sanitary sewer networks by starting from the most upstream
102 pipes, iteratively working downstream, and designing each pipe by minimising the costs
103 subject to the feasibility of design constraints; such an approach could be equally valid for a
104 UDM. In cases where the impervious contributing area of a given pipe has been
105 synthesised, a Rational Method could be applied for determining pipe size. A variety of more
106 extensive global optimisation methods exist for hydraulic design to both minimise costs (e.g.,
107 Sun et al., (2011)), or calibrate to observations (e.g., Huang et al., (2022); Sytsma et al.,
108 (2022)). However, these calibration studies highlight the inherent equifinality in parameter
109 selection, thus suggesting the uncertainties in such a high dimensionality problem may
110 outweigh any 'optimal' algorithm.

111 Because UDM synthesis requires a hydraulic design, equifinality must also be inherent to
112 UDM synthesis. We argue that this has been under-recognised in existing UDM synthesis,
113 primarily because of a lack of data and the absence of an automated, end-to-end workflow to
114 assess the impact of parameter selection. A reader may observe results from the
115 supplement of Duque et al., (2022), which demonstrates that small changes in their grid
116 scale for the synthesis algorithm can generate dramatically different sanitary sewer
117 networks.

118 An equally valid line of inquiry is, therefore, to examine UDM synthesis with sensitivity
119 analysis to quantify the importance of various factors in generating more realistic networks
120 (Pianosi et al., (2016). Sensitivity analysis provides verification by revealing ranges of
121 'behavioural' parameter values that produce acceptable model outputs, thus informing
122 application of UDM synthesis in data-sparse regions. Additionally, it reveals the dominant

123 controls and key processes governing UDM synthesis by quantifying the relative importance
124 of different parameters. In turn, revealing where uncertainty reduction may be most
125 beneficial. We do not assume that accurate UDM synthesis is possible in every location
126 using solely building, road, and elevation data, particularly given the complexities involved in
127 the gradual expansion of a UDM (Rauch et al., 2017). However, it is impractical to improve
128 UDM synthesis by capturing every possible element involved in network evolution. Instead,
129 sensitivity analysis provides an objective way to guide improvement; prioritising
130 measurements and processes that relate to the most sensitive parameters.

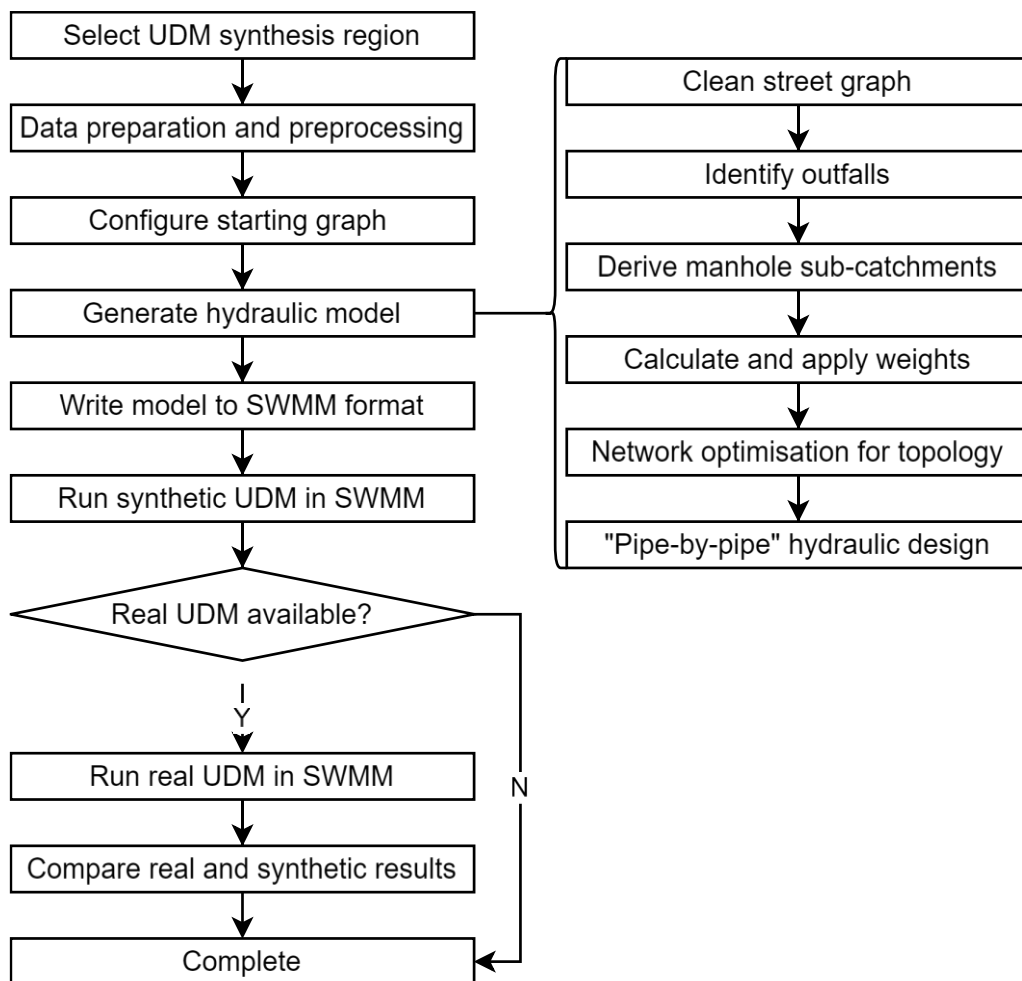
131 Continual improvements in development and accessibility of remote sensing and open
132 geospatial data at global scale facilitates applicability of UDM synthesis in many locations.
133 Chegini et al., (2022), demonstrate an approach that can perform network topology and the
134 dimensioning part of hydraulic design anywhere in the continental United States. Montalvo et
135 al., (2024) implement the UDM synthesis algorithm presented by Reyes-Silva et al., (2023),
136 in a GIS tool, however this approach does not acquire/process the necessary geospatial
137 data nor is it open-source at time of writing. We believe that a global tool, that is open-
138 source, and tailored to accommodate the uncertainty inherent in the UDM synthesis problem
139 would be of great value to the urban drainage community. Such a tool would enable
140 hydrodynamic method developers to bypass the reproducibility crisis (Stagge et al., 2019;
141 Hutton et al., 2016), by demonstrating their tools on an unlimited suite of UDMs synthesised
142 in cities worldwide, improving on the entirely theoretical test suites that presently exist
143 (Möderl et al., 2011, 2009; Sweetapple et al., 2018). Furthermore, it would contribute
144 towards better representation of urban environments in the regional hydrological cycle,
145 which is a critical and under-represented component of such applications (Coxon et al.,
146 2024).

147 In this paper we present a workflow, called SWMManywhere, to synthesise UDMs anywhere
148 in the world. We show its versatility by applying it to multiple case studies (i.e. sewer
149 systems of different sizes in two different countries) and to facilitate its global usage we

150 deploy it as an open-source Python tool (Dobson et al., 2024a) with extensive
 151 documentation (SWMManywhere documentation, 2024). SWMManywhere provides a
 152 parameterised and easy to customise approach for UDM synthesis which allows us to
 153 perform sensitivity analysis of synthesised UDMs. We ensure SWMManywhere responds to
 154 the need for worldwide application by using open global datasets and including the retrieval
 155 and preprocessing of these datasets as part of the algorithm. The methods implemented in
 156 SWMManywhere also include a variety of technical novelties in the field of UDM synthesis,
 157 including use of a minimum spanning arborescence to derive topology, enabling
 158 minimisation of contributing area during this process, and implementing Duque et al.,
 159 (2022)'s pipe-by-pipe design method for urban drainage networks.

160 2 Methodology

161 A high-level overview of our proposed SWMManywhere workflow is shown in Figure 1.



162

163 *Figure 1: Overview of the SWMManywhere workflow.*

164 We present an end-to-end workflow for UDM synthesis and comparison against a real UDM,
165 if available, anywhere in the world. A key barrier to UDM synthesis identified in literature is
166 difficulty in setting up a hydraulically correct model, thus we specify data acquisition and
167 preprocessing in the workflow. The 'generate hydraulic model' step, is the key step that
168 should ultimately create sub-catchments, a network topology, and hydraulic designs of pipes
169 that together fully describe the synthesised drainage network. Such a drainage network, i.e.,
170 the synthetic UDM, will be valid for simulation in a widely used software for design and
171 analysis of drainage networks, such as SWMM, enabling studying different precipitation
172 events and inspecting state variables such as pipe flows and pluvial flooding. In Section 2.1,
173 we describe the theory and processes in our workflow, also explaining how it can be
174 customised with parameter choices and additional processes to vary the nature of the
175 synthesised UDM.

176 A key hypothesis that must underlie any synthetic UDM approach is that results may be valid
177 in places where a real UDM is not available or not trusted. Because we observed the
178 sensitivity to parameter selection in previous UDM synthesis literature, we intentionally
179 specify SWMManywhere to be highly parameterised and customisable. We use sensitivity
180 analysis on these parameters to demonstrate how they impact synthesised networks. In
181 Section 2.2, we describe how sensitivity analysis can guide the use of SWMManywhere in
182 areas where parameters cannot be estimated a priori based on field data and provide a
183 deeper understanding of UDM synthesis. We apply this analysis to eight UDMs in two
184 different locations.

185 We discuss UDM synthesis using graph theory terminology:

- 186 • A graph represents the UDM, consisting of nodes (manholes) that are connected by
187 edges (pipes). The graph can be either undirected or directed, indicating that
188 connections are between two nodes (undirected) or from one node to another
189 (directed). Pipes are undirected since head may drive uphill flow, however, treating

190 the graph as directed enables better description of preferential flow paths and is also
191 the format required by SWMM, SWMMAnywhere makes use of both directed and
192 undirected graphs.

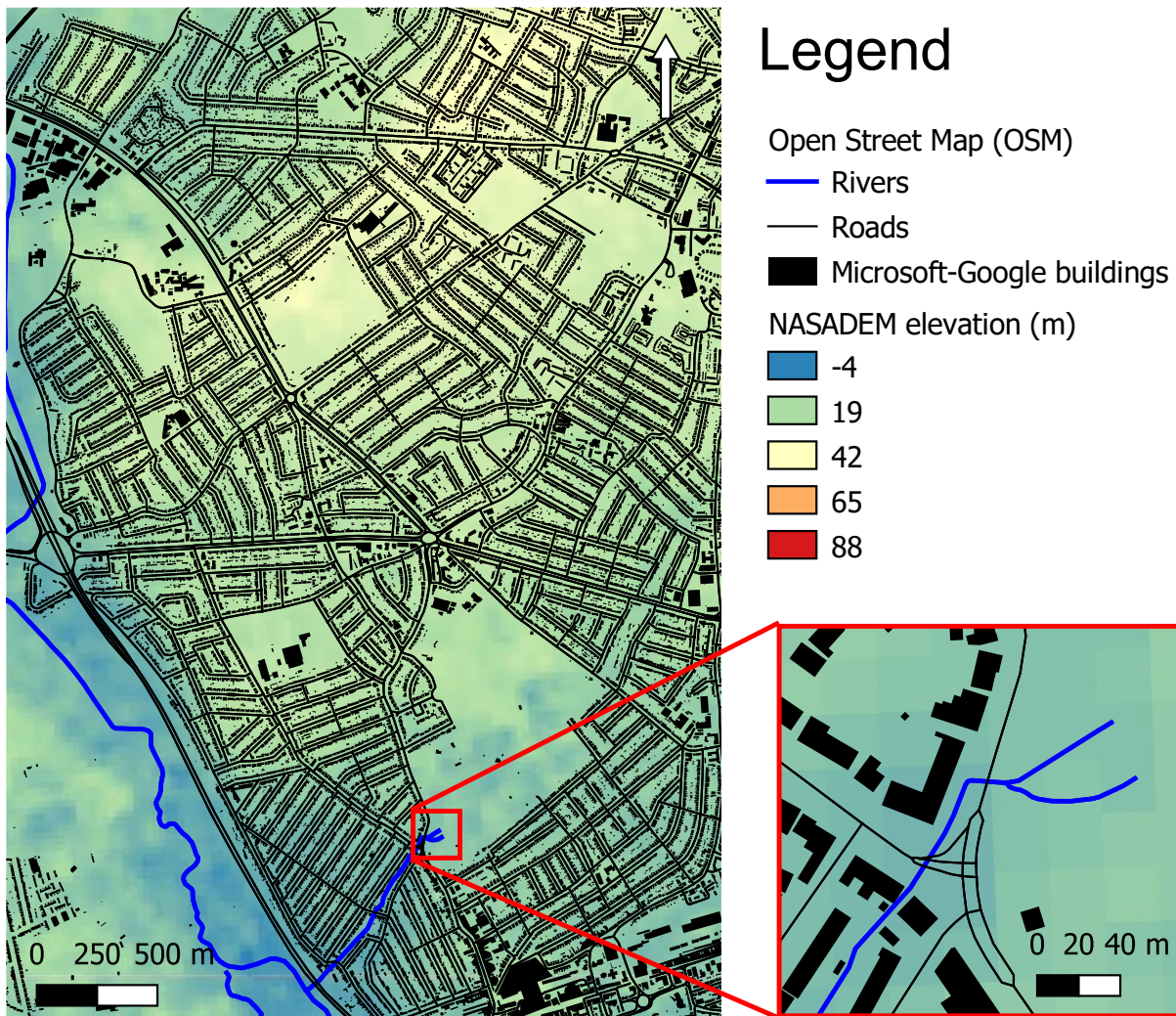
- 193 • In graph theory, a subgraph refers to a sub-selection of the graph and is called a
194 connected component if every node is in the subgraph reachable from every other
195 node within that subgraph. Connected components are used in SWMMAnywhere to
196 describe a collection of manholes and pipes that drain to a common outfall.
- 197 • The topology of the graph captures the overall arrangement and relationships of
198 nodes and edges and can be thought of as the pipe layout in a UDM. The edges can
199 have costs, for example length, which may be minimised by shortest path algorithms
200 to minimise flow routes. Flow routes should be minimised in any drainage network to
201 drain the catchment as efficiently as possible, preventing the accumulation of water
202 and flooding of manholes. A minimum spanning tree is a subgraph that connects all
203 nodes with the minimum possible total edge cost for an undirected graph, a minimum
204 spanning arborescence is the same for a directed graph, thus these represent the
205 most cost-efficient pipe layouts that may exist for a given area. We will refer to a
206 graph of potential pipe-carrying edges as the street graph, while the optimised layout
207 is the UDM topology.

208 2.1 SWMMAnywhere

209 2.1.1 *Data and preparation*

210 Our SWMMAnywhere approach uses datasets that are of sufficient level of detail to be used
211 in global application: road locations, river locations, elevation, and building footprints. We
212 stress that these datasets, in particular road locations and building footprints, vary in quality
213 from location to location, thus, the downloaded data for a given case study should always be
214 inspected carefully. Additionally, we enable manually sourced, higher quality data for input, if
215 available, as described in the online documentation (SWMMAnywhere documentation,

216 2024). The default datasets are visualised for one of our case studies in Figure 2, and
217 described in further detail in this section.



218

219 *Figure 2: Visualisation of downloaded data in the Cran Brook, UK. See main text for citations.*

220 *Streets and rivers*

221 Assuming pipes can only exist in pre-specified plausible locations will dramatically reduce
222 the dimensionality of the shortest-path UDM topology derivation. Thus, we assume that
223 pipes can only exist in certain locations, typically streets due to the common validity of this
224 assumption (Mair et al., 2017). In addition, paved streets constitute one of the key
225 impervious surfaces which must be drained in a UDM. Rivers are also downloaded as these
226 are potential outfall locations of the drainage network, described in further detail in Section

227 2.1.2. OpenStreetMap (OSM) provides street and river data worldwide and is used in this
228 study.

229 *Impervious areas*

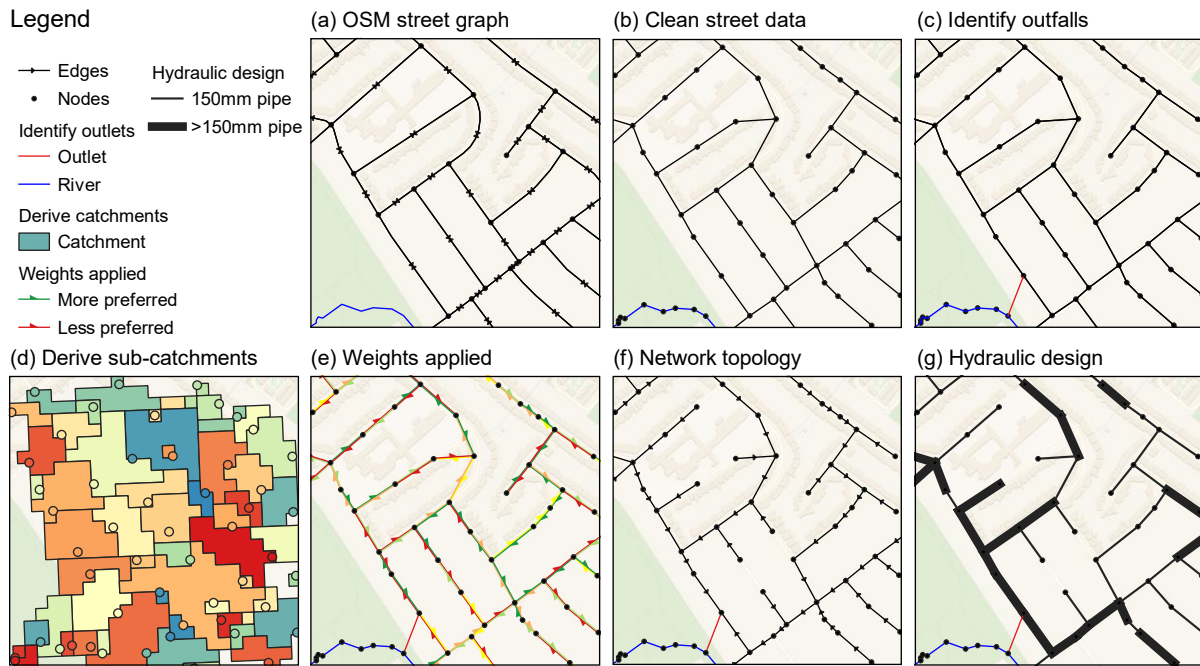
230 To calculate the impervious area of a sub-catchment, and thus enable runoff generation, we
231 use road locations, their number of lanes, which are contained within OSM, and building
232 footprints. Recent advances in machine learning have enabled identification of building
233 perimeters from high-resolution satellite data worldwide. Two large datasets, provided by
234 Google and by Microsoft, are now combined and available at (Google-Microsoft Open
235 Buildings, 2024). Both datasets use convolutional neural networks to classify pixels as
236 buildings (Tan and Le, 2019; Sirko et al., 2021) and custom methods to polygonise these
237 pixels into buildings (Sirko et al., 2021; Computer generated building footprints for the United
238 States, 2024). The authors would note that, although global, this dataset has varying quality
239 in different regions due to the nature of the training data that was used and resolution of
240 satellite imagery. Although other impervious surfaces besides roads and buildings, such as
241 car parks, that must be drained in a UDM are common, we could not identify global datasets
242 describing these, and thus consider them currently outside the scope of this study.

243 *Elevation*

244 Elevation data, in the format of a Digital Elevation Model (DEM), is essential to delineate
245 manhole sub-catchments, to calculate the slope along edges, and to identify if there are
246 paths in the street graph that should not be ignored, for example, those at that span different
247 hydrological catchments. We use NASADEM, which is a publicly available radar-based
248 global DEM at 30m resolution (Crippen et al., 2016), from Microsoft Planetary Computer
249 (Source et al., 2022). Although higher resolutions around 2m are recommended for UDM
250 (Arrighi and Campo, 2019), such datasets do not yet exist openly at global scales.

251 2.1.2 Pipe network generation

252 A key innovation of our approach is to iteratively process a street graph and gradually
253 transform it into a UDM with full hydraulic design. These processes must take a graph and
254 return a graph. The key tasks that they perform are summarised in Figure 3, discussed
255 further in this section and used for the experiments in this paper.



256

257 *Figure 3: Visualisation of key iterations to the graph as different processes are applied. Catchments (D) are*
258 *coloured by the manhole that they drain to.*

259 Table 1 lists all tuneable parameters of our proposed workflow, with reasonable default
260 values for these parameters and their ranges provided in the online documentation
261 (SWMManywhere documentation, 2024). We carry out an extensive sensitivity analysis (see
262 Section 2.2) to identify any behavioural ranges of these parameters and identify their relative
263 importance in UDM synthesis.

264
265
266

Table 1: SWMManywhere user adjustable parameters that are tested in sensitivity analysis for this work, a full list of parameters is available in the online documentation (SWMManywhere documentation, 2024). If the variable is described differently from its use in the software to improve clarity, the software term is indicated in brackets.

GROUP	VARIABLE	KEY
SYSTEM DESCRIPTION (MANHOLES AND OUTFALLS)	node merge distance	pNM
	outfall length	pOL
	max street length	pXS
	river buffer distance	pRB
TOPOLOGY DERIVATION	chahinian slope scaling	pSS
	chahinian angle scaling	pAS
	length scaling	pLS
	contributing area scaling	pCS
	chahinian slope exponent	pSE
	chahinian angle exponent	pAE
	length exponent	pLE
	contributing area exponent	pCE
HYDRAULIC DESIGN	max filling ratio (max fr)	pFR
	min v	pMV
	max v	pXV
	min depth	pMD
	max depth	pXD
	design precipitation (precipitation)	pDP

267

268 *Data cleaning and manhole identification*

269 As explained in Section 2.1.1, OpenStreetMap (OSM) is the default data source for obtaining
 270 street and river graphs. However, the raw OSM data are not directly suitable for UDM
 271 generation, so we perform a variety of data cleaning operations to create a more suitable
 272 graph for UDM synthesis, as illustrated in Figure 3a-b. The first significant process in data
 273 cleaning is enforcing a maximum edge length, splitting edges that are longer than max street
 274 length parameter (*pXS*, Table 1). The second is merging of nodes, which joins nodes
 275 together if they are within a specified distance of each other (*node merge distance*, *pNM*).
 276 These two processes jointly control where manholes are located along edges and the
 277 frequency with which they occur. The final significant task in data cleaning is buffering street
 278 paths in proportion to the number of lanes to create a shapefile of impervious street area.
 279 The remainder of processing in this stage is perfunctory, performing tasks such as ensuring
 280 consistent geometries, a consistent identification scheme, removing parallel edges, and

281 converting the directed street graph to an undirected graph (as a pipe may flow in a direction
282 opposite to road travel).

283 *Sub-catchment outline and surface characteristics*

284 We begin the sub-catchment delineation, by first burning the road network into the DEM of
285 an urban area. This burning process is a common practice in UDM sub-catchment
286 representation (Gironás et al., 2010) and involves lowering the elevation of grid cells in the
287 DEM that contain roads. Then, we hydrologically condition the DEM by breaching
288 depressions (Lindsay, 2016a). Upon conditioning the DEM, we compute the flow direction,
289 using the D8 method (O'Callaghan and Mark, 1984), and slope. Because our workflow
290 includes generation of a SWMM model, a sub-catchment width parameter is required. We
291 follow the approach proposed by InfoWorks (Subcatchment Data Fields (InfoWorks), 2024)
292 to compute the width of a sub-catchment based on the radius of a circle with area equal to
293 the area of the sub-catchment.

294 *Outfall identification*

295 Another key feature of a UDM is outfall locations. The first step in identifying outfalls requires
296 assessing the topology of the graph to ensure its hydrologic feasibility (Seo and Schmidt,
297 2013; Li and Willems, 2020). To achieve this, we remove edges that cross the boundaries of
298 hydrological catchments (defined as the largest non-overlapping drainage basins in the
299 study region), because these are unlikely to carry a pipe. Then, we identify potential outfall
300 locations by assuming that outfalls may only exist within a specified distance of a river (*river*
301 *buffer distance, pRB*). Although other factors such as environmental considerations affect
302 selection of the outfall location, in this study, we only account for the vicinity of water bodies.
303 We incorporate the relative construction cost of outfalls in our workflow, by assigning weights
304 to the identified outfall locations based the length of the pipe that connects the network to
305 the river (*outfall length, pOL*). If no potential outfalls are identified the node with the lowest
306 elevation is used as the outfall. On the other hand, in cases where multiple plausible outfalls

307 are identified, we retain them all at this step and determine the outfall during the network
308 topology derivation step.

309 *Calculating weights and network topology*

310 The network topology can be derived as a minimisation problem of overall graph cost. This
311 minimisation should start with a graph of potential edges (i.e., the graph up to this point) and
312 return a directed graph that visits all nodes (manholes), minimising overall graph cost,
313 without retaining redundant edges (pipes), which is also referred to as a minimum spanning
314 arborescence (MSA).

315 The first step to take in network topology derivation is to identify how each edge contributes
316 to the overall graph cost. As identified by Chahinian et al., (2019), it is plausible that each of
317 pipe length, pipe slope and pipe adjacent angle (the angle at which two joining pipes meet)
318 are important to consider for minimisation. We further propose that the total contributing area
319 carried by pipes in the derived network should also be minimised. As with *ibid.*, these factors
320 do not necessarily contribute to the overall graph cost symmetrically or proportionally. For
321 example, while both negative slopes and overly steep positive slopes are penalised, the
322 penalisation on negative slopes increases with slope more sharply than for positive slopes,
323 because the former becomes hydraulically impractical more quickly than the latter. It is not
324 apparent which of these factors (slope, angle, area, and length) are more important to
325 minimise than others and so we combine each factor to be varied, as in *ibid.* We deviate
326 from *ibid.* by assigning both a linear and exponential scaling parameter to each factor (rather
327 than solely linear), enabling high customisation of how overall graph cost is calculated (i.e.,
328 parameters in the *topology derivation* group). We calculate each individual factor, apply
329 scaling parameters, and sum these into an overall cost for each edge in the graph,
330 producing a graph such as that visualised in Figure 3e.

331 The network topology is then derived using an implementation based on the shortest-path
332 algorithm proposed by Tarjan (1977), to find the MSA of the graph. The algorithm starts from

333 a designated "waste" node that all potential outfall locations are connected to, either directly
334 or through river paths, thus enabling all connected component subgraphs to be handled in a
335 single pass. The algorithm initializes a priority queue with the waste node's incoming edges,
336 sorted by their costs. At each step, the minimum cost edge is extracted from the priority
337 queue. If the node it leads to is not already included in the arborescence being constructed,
338 that node and edge are added to the arborescence. The node is marked with its parent, and
339 any edges incoming to that node are added to the priority queue. This process continues
340 until all nodes are included in the arborescence. The final arborescence represents the UDM
341 network topology, where the selected edges correspond to the pipe segments that must be
342 hydraulically designed.

343 *Hydraulic design*

344 Duque et al., (2022), propose a "pipe-by-pipe" method to design sanitary sewer network
345 pipes, the method starts at the most upstream pipes, designing each pipe in terms of
346 diameter and depth under a set of design constraints (see *hydraulic design* group), and
347 continues iterating downstream. They demonstrate that this method is comparable to an
348 optimal dynamic programming-based approach, although is significantly more efficient. We
349 adapt the pipe-by-pipe approach to make it suitable for a SWMManywhere approach:

- 350 • Rather than deriving the design flow from household waste generation, we use a
351 Rational method that calculates the design flow as the entire impervious area in sub-
352 catchments upstream of the pipe being designed multiplied by a *design precipitation*,
353 *pDP*, amount.
- 354 • Inspection of any large real UDM will commonly reveal pipes travelling in an uphill
355 direction, as measured by surface elevation. Wherever possible the pipe's elevation
356 will be such that they flow downhill despite the surface elevation, however there is no
357 guarantee that any hydraulically feasible design will exist. Because Duque et al.
358 (2022) derive network topology using hydrological flow paths a feasible design will
359 always exist, however this is not the case for SWMManywhere, which uses streets

360 for pipe locations and accounts for factors besides slope during network topology
361 derivation. To accommodate this, we include a surcharge feasibility constraint, which
362 allows a pipe to be designed for flow under surcharge, provided this is the only way
363 to reach a feasible hydraulic design.

- 364 • To provide better performance, we assess all designs for a pipe rather than selecting
365 the first feasible design. The selected design first aims to satisfy feasibility
366 constraints, and if no feasible design exists, picking the most feasible design. It then
367 minimises depth, diameter, and excavation cost, as calculated in Duque et al. (2022).

368 The final product is a fully described UDM, complete with sub-catchments and hydraulic
369 designs, thus sufficient to be simulated in software such as SWMM.

370 *2.1.3 Measuring effectiveness of UDM synthesis*

371 The question of ‘how realistic is a synthesised UDM’ is most sensibly assessed by
372 comparing synthesised results against a real UDM. UDM synthesis in a sensitivity analysis
373 context requires understanding why we see the results that we see. Thus, an extensive suite
374 of allowable performance metrics is provided covering a variety of different measures and
375 variables, see Table 2 for a list of the metrics used in this study. We define metrics that
376 measure performance for different elements of UDM synthesis. System description metrics
377 assess the synthesised UDM in terms of properties that describe infrastructure, topology
378 metrics investigate the layout of the graph, and design metrics assess the derived diameter
379 of pipes. Furthermore, the UDM is simulated in SWMM and thus simulated flow, and flooding
380 can also be compared.

381 *Table 2: List of metrics implemented in SWMMAnywhere*

CATEGORY	MEASURE	VARIABLE	KEY
SYSTEM DESCRIPTION	relerror	length	mRL
	relerror	npipes	mRP
	relerror	nmanholes	mRM
TOPOLOGY	deltacon0	-	mD0
	laplacian distance	-	mLD
	vertex edge distance	-	mVD
	kstest	edge betweenness	mKE
	kstest	node betweenness	mKN
DESIGN	relerror	diameter	mRD
	kstest	diameter	mKD
SIMULATION	nse	flow	mNQ
	kge	flow	mKQ
	relerror	flow	mRQ
	nse	flooding	mNF
	kge	flooding	mKF
	relerror	flooding	mRF

382 Comparing flow and/or flooding simulations is typical in the UDM synthesis literature (Reyes-
 383 Silva et al., 2023; Blumensaat et al., 2012). We create a timeseries of total flooded volume to
 384 assess flooding simulation performance across the entire network. Meanwhile, flows are
 385 assessed at the system outfall, as with (Blumensaat et al., 2012). However, unlike existing
 386 literature, which assumes that the outfall locations of the network being synthesised are
 387 known, we do not make this assumption, as this information is not globally available.

388 Instead, we identify where synthetic manholes fall inside sub-catchments of the real network.
 389 From these classified manholes it identifies the most commonly represented outfall, and sub-
 390 selects only that connected component for comparison purposes.

391 Because the reasons for performing sensitivity analysis are to understand how parameters
 392 change behaviours in UDM synthesis, the most common measure of performance we use is

393 the relative error (*relerror* measure in Table 2, equation 1), which is simple to understand
394 and provides directionality in terms of over/under estimation,

$$relerror = \frac{mean(synthetic) - mean(real)}{mean(real)} \quad (1),$$

395 where *synthetic* is the synthetic UDM data to be compared against the *real* data. We omit a
396 conventional *time* component of the metric because the same equation can equally be used
397 for timeseries or design properties (such as average diameter) alike. In cases of comparing
398 flow or flooding timeseries, we also include the Nash-Sutcliffe Efficiency and Kling-Gupta
399 Efficiency, because these are commonly used and so will provide users who are familiar with
400 them a more nuanced grasp of the synthetic UDM's performance.

401 A further set of measures that can be used for synthetic networks are those that test the
402 topological similarity of the derived vs real network, we implement a variety of those
403 presented in existing literature (Wills and Meyer, 2020; Chegini and Li, 2022), see *topology*
404 category in Table 2.

405 2.1.4 Implementation

406 SWMManywhere is a highly modular workflow and in this study, we implement it in Python
407 and publish it as an open-source tool (Dobson et al., 2024a). We note that the workflow is
408 general and can be implemented in any other programming language. In our implementation
409 of SWMManywhere the minimal required user input is the bounding box of the target urban
410 area, and all remaining steps Figure 1 are automated. The bounding box should be provided
411 in terms of latitudes and longitudes in WGS 84 geographic coordinate system (EPSG:4326).
412 SWMManywhere will reproject all downloaded data into the Universal Transverse Mercator
413 (UTM) coordinate system. UTM uses a coordinate system with metre as its unit, and thus
414 can provide accurate distance and area calculations in contrast to WGS 84. The UTM is split

415 into zones and the zone ultimately used in a SWMManywhere run is calculated based on the
416 UTM zone of the bounding box.

417 As we described in Section 2.1.2 the most complex step in the workflow is the pipe network
418 generation, i.e., iteratively applying various graph operations to the initial graph street to
419 generate the final UDM. These operations, referred to in our implementation as graph
420 functions, have a variety of parameters that need to be specified, as listed in Table 1.
421 Considering the importance of graph functions and to accommodate flexibility in applying
422 them, our implementation allows adding, removing, or changing their order without modifying
423 the code. Structuring code into graph functions enable easy reuse of code, customisation,
424 and introduction of new processing steps. Graph functions are wrapped in a class for
425 validation, enabling SWMManywhere to identify if a set of graph functions to be applied is
426 valid *a priori*. Graph functions are stored in a registry object to enable easy access. We
427 provide a description of all graph functions in the documentation online (SWMManywhere
428 documentation, 2024). However, users may also customise the selection and order of graph
429 functions, or create new ones, as described in the online documentation, to fit their
430 requirements.

431 Processes or operations described in Sections 2.1.1 and 2.1.2 that are used by but not
432 implemented natively within the tool are described in Table 3.

433 *Table 3: List of tools for specific tasks in our SWMManywhere implementation.*

TASK	SOFTWARE	REFERENCE
DEM CONDITIONING	Whitebox	(Lindsay, 2016b)
FLOW DIRECTION CALCULATIONS	Whitebox	(Lindsay, 2016b)
SUB-CATCHMENT DELINEATION FROM FLOW DIRECTIONS	PyFlwDir	(Eilander, 2022)
SUB-CATCHMENT SLOPE CALCULATION	PyFlwDir	(Eilander, 2022)
OSM DATA RETRIEVAL	OSMnx	(Boeing, 2017)
GRAPH OPERATIONS	Networkx	(Hagberg et al., 2008)

434

435 To accommodate ease of use for a wide range of users with different levels of programming
 436 experience, we provide a command-line interface (CLI) for the software. More experienced
 437 users can take advantage of the modularity of SWMManywhere for more advanced
 438 customisation of the workflow. The CLI works with a configuration file that enables a user to
 439 change parameter values and functionality. The minimal essential requirements that this file
 440 must contain are a project name, a base directory, and a bounding box. The configuration
 441 file provides a centralised location to perform customisations including changing the
 442 selection/ordering of graph functions, changing parameter values (see Table 1), file locations
 443 of a real network to compare against (see Section 2.1.3) and which metrics to calculate (see
 444 Table 2), a starting graph if not using downloaded street data, and any running settings for
 445 the SWMM simulation. A variety of online tutorials explain the procedure to make such
 446 customisations.

447 SWMManywhere provides a capability to write simple SWMM model files (typically with a
 448 .inp file extension) that have been synthesised via the various graph functions used. It also
 449 provides a wrapper of the PySWMM software (McDonnell et al., 2020), which enables calling
 450 the SWMM software and interacting with its simulations from Python. Thus, in addition to the

451 UDM synthesis, writing, running, and calculating metrics if real network information exists
452 are carried out during the command line call.

453 Precipitation data is frequently identified as a critical factor in UDM simulations (Ochoa-
454 Rodriguez et al., 2015), however, there are currently no open global datasets that provide
455 the high frequency monitoring needed to drive these models and so precipitation must be
456 user-provided if deviating from the default storm provided as part of the tool.

457 2.2 Sensitivity analysis

458 Sensitivity analysis is used to examine how output variations can be attributed to input
459 variations, typically expressed as sensitivity indices for each model parameter (Pianosi et al.,
460 2016). While popular reviews in the environmental sciences define sensitivity analysis as
461 specific to model input/outputs (Saltelli et al., 2008, 2019; Pianosi et al., 2016), it can equally
462 be applied to any generic parameterised workflow, such as SWMMAnywhere. As defined in
463 Table 1, there are a wide variety of parameters that must be selected, many of which do not
464 have values that could be easily measured or derived, and thus are useful candidates for
465 sensitivity analysis.

466 In general, it is recognised that, to robustly conduct sensitivity analysis, a global method
467 should be used, and the variability of the calculated indices should be checked to ensure
468 that the number of samples is sufficient (Saltelli et al., 2019). Because of the presumed high
469 level of dependency in the SWMMAnywhere workflow (for example, hydraulic design
470 depends entirely on network topology, which in turn depends on outfall and manhole
471 identification), we also calculate second order indices to better capture interactions between
472 parameters (Herman and Usher, 2017). To implement sensitivity analysis for
473 SWMMAnywhere, we use the SALib software (Herman and Usher, 2017), which provides a
474 variety of global methods for sampling parameter ranges and calculating sensitivity indices
475 natively in Python. In this study we use the Sobol method (Sobol, 1993) due to its
476 widespread use and recognised robustness of results providing that a sufficient number of
477 samples can be investigated (Pianosi et al., 2016). 18 parameters are sampled, indicated in

478 Table 1, and 16 metrics, Table 2, are evaluated. Thus, the overall approach is to perform
479 parameter sampling, run SWMMAnywhere with the parameters of each sample, calculate the
480 performance metrics between the synthesised and real UDMs, and calculate sensitivity
481 indices.

482 Sobol sensitivity analysis that includes second order interactions with SALib requires taking
483 samples equal to,

$$N = n * (2m + 2) \quad (2),$$

484 where N is the total number of samples (or SWMMAnywhere calls), m is the number of
485 parameters, and n is the number of Sobol sequence samples to generate (preferably a
486 power of 2). In this experiment we set n to 2^{10} (1024), m is 18, resulting in N of 38912. As
487 demonstrated in Pianosi et al., (2016), this many evaluations ($m * 1000$) are towards the
488 upper limit of what is found in the literature. We take this opportunity to note a further benefit
489 of sensitivity analysis in the context of SWMMAnywhere as a global tool, which is that testing
490 it under such a large and diverse range of parameters further guarantees robustness of the
491 software implementation in locations not tested.

492 **3 Case studies**

493 In this study, we evaluate our proposed workflow by comparing the SWMM simulation
494 results obtain from using the synthetic UDM with those of the real UDM for the Cran Brook,
495 London, UK (Babovic and Mijic, 2019). We then perform sensitivity analysis in other
496 locations to examine the transferability of results and parameters. We use seven UDMs
497 around the town of Bellinge, Denmark, as delineated by Farina et al., (2023). These data
498 were selected because they are openly available and demonstrate results over a wide range
499 of scales (Pedersen et al., 2021). The properties of the case study networks are presented in
500 Table 4.

501 *Table 4: Summary of networks tested and their properties*

Network	Number of nodes	Number of edges	Impervious percentage
Cran Brook	6931	6965	27
Bellinge 1	142	150	36
Bellinge 2	118	117	33
Bellinge 3	52	51	25
Bellinge 4	46	45	32
Bellinge 5	45	46	40
Bellinge 6	36	35	32
Bellinge 7	15	14	34

502

503 A key feature of many UDM is the presence of hydraulic structures such as weirs, orifices,
 504 storages, or pumps. There is extensive evidence from the sewer network simplification
 505 literature that capturing and parameterising these structures is critical towards reproducing
 506 the behaviour of the real network (Thrysoe et al., 2019; Dobson et al., 2022). However,
 507 SWMManywhere currently does not attempt to estimate the locations or hydraulic properties
 508 of any such structures. We acknowledge that this could be a significant limitation and hope
 509 to add this behaviour in future work. In this paper, we replace the hydraulic structures and
 510 storage nodes in the real models with simple and uniform nodes to better assess the
 511 SWMManywhere workflow as designed. Furthermore, the hydraulic properties of sub-
 512 catchments (specifically, the Manning’s roughness coefficient and depression storage of
 513 both impervious and pervious areas) are a significant source of uncertainty and typically
 514 calibrated or set arbitrarily (Deletic et al., 2012), thus we set these at the same values for all
 515 networks to ensure comparability.

516 The precipitation event we use to demonstrate SWMManywhere is the largest storm in the
 517 openly available Bellinge data (Pedersen et al., 2021).

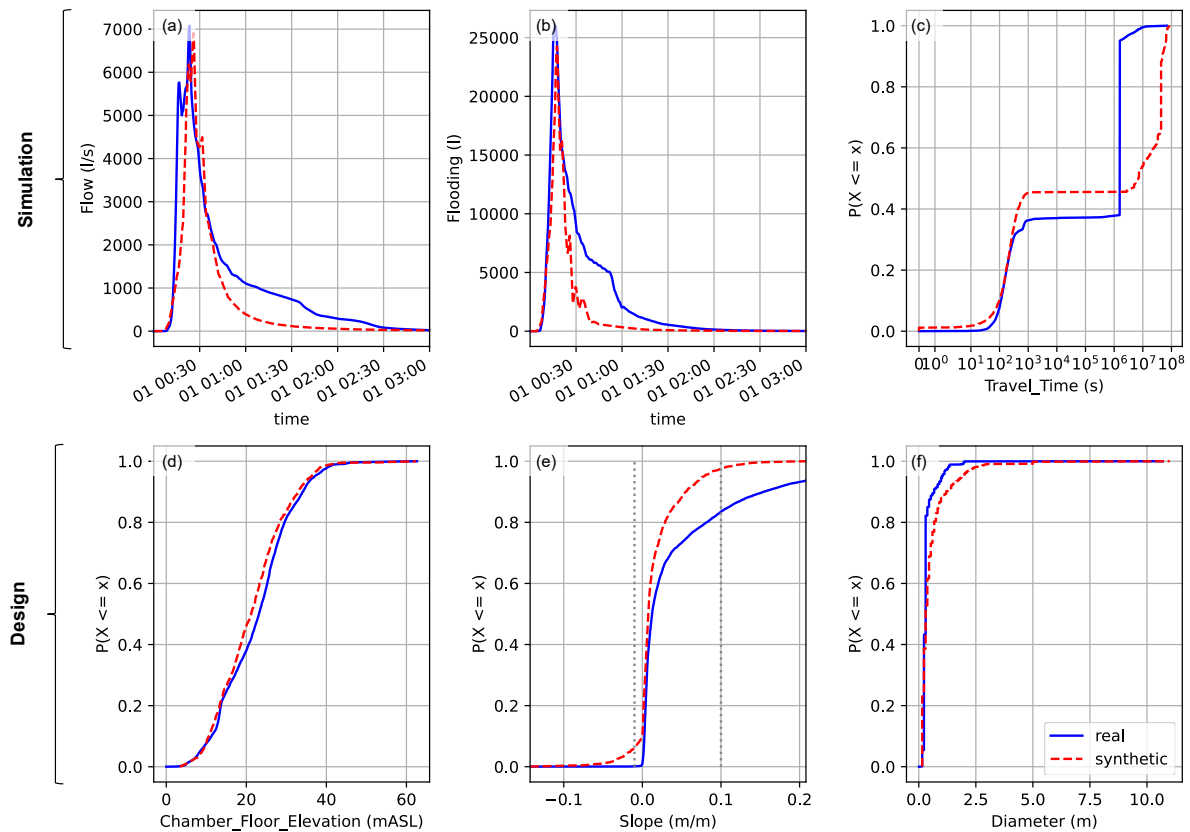
518 Workflow evaluations were performed on the Imperial College High Performance Computing
519 facilities (see Acknowledgements). Hardware used was typically AMD EPYC 7742 (128
520 cores, 1TB RAM per node), although this varied based on availability. On one of these
521 machines, for a single workflow evaluation in the Cran Brook case study, downloading and
522 data preprocessing takes ten seconds (except for buildings, which are national datasets and
523 so download speeds will vary significantly depending on the country), evaluating graph
524 functions and writing the UDM to SWMM format takes around two minutes (deriving sub-
525 catchments and deriving network topology are the slowest individual steps at 20 seconds
526 each), simulation in SWMM takes eight minutes, and evaluating metrics takes two minutes
527 (dominated by the *K-S test for node betweenness, mKN* which took over one minute). Run
528 times for all Bellinge case studies were dramatically quicker owing to the far smaller UDM
529 sizes.

530 The code used to perform this experiment and results required to reproduce the figure
531 results in Section 4 are openly shared in a separate repository (Dobson et al., 2024b).

532 **4 Results**

533 4.1 Proof-of-concept examination

534 We focus this section on a synthesised model selected from our sensitivity analysis sampling
535 (Section 4.2) that performed well across a range of metrics to assess SWMManywhere's
536 ability to generate a high-quality UDM and raise methodological points of interest. Figure 4
537 plots a flow and flooding timeseries and diameter, elevation, slope, and travel time
538 distributions for the Cran Brook network to provide a detailed comparison of the real and
539 synthetic UDM.



540

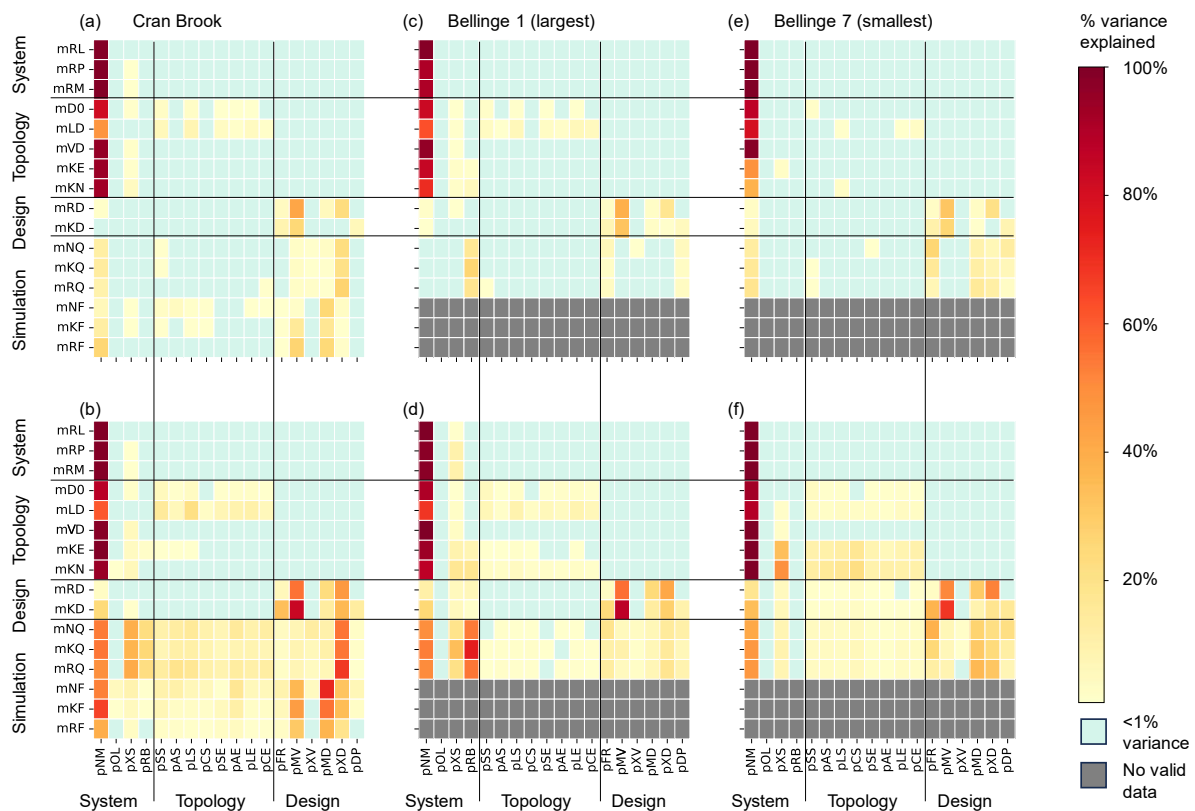
541 *Figure 4: Demonstration plot of a high performance synthetic UDM. Red dashed lines represent synthetic data,*
 542 *while solid blue represents the real UDM simulations. Grey lines on the slope plot (e) show the target design*
 543 *range.*

544 Figure 4a shows flow at the network outfall, while Figure 4b shows the total flooded volume
 545 across the network. We see that the maximum values of both are captured with accuracy,
 546 however, the falling limb for both recedes more quickly in the synthetic network than in the
 547 real UDM simulations. The synthetic network has consistently larger diameters (Figure 4f)
 548 than the real, while chamber floor elevations (Figure 4d) are well matched. Synthetic pipe
 549 slopes (Figure 4e) are lower, although we observe that these are primarily within the grey
 550 dashed lines which show the target design range (Chahinian et al., 2019). The average
 551 travel time from each node to the outfall (Figure 4c) shows distinctively different patterns
 552 across the distribution, with a good match for the quickest third of nodes, the synthetic UDM
 553 quicker for the middle third (because of the larger diameters), and the real UDM quicker for
 554 the slowest third. Although not shown, the total runoff from manhole sub-catchments in both

555 the real and synthetic models is within 2% of each other, which is true for all synthesised
 556 UDMs.

557 4.2 Sensitivity analysis, Cran Brook

558 SWMMAnywhere parameters, see Table 1, were sampled using a Sobol sampling scheme,
 559 see Section 2.2, to enable a global sensitivity analysis using the Sobol method. The findings
 560 of this analysis for Cran Brook, the sensitivity indices, are presented in Figure 5a-b. Two
 561 other locations (Figure 5 c-f) are discussed in Section 4.2, with other locations in full
 562 presented in Supplemental Figure S1.



563
 564 *Figure 5: Heatmap demonstrating the sensitivity indices (a) of first order variance (S1) of a metric (y-axis)*
 565 *attributable to a parameter (x-axis) based on simulations in the Cran Brook network, (b) of total variance (ST)*
 566 *attributable to a parameter based on simulations in the Cran Brook network. Red indicates more sensitive and*
 567 *yellow less sensitive. Blue indicates less than 1% variance explained. (c, d, e, f), shows equivalent of (a) and (b)*
 568 *respectively, but for the Bellinge 1 and Bellinge 7 networks. Grey indicates no sensitivity indices could be*
 569 *calculated because no flooding occurred.*

570 In Figure 5 we show the first order variance (S1) of each metric (as listed in Table 2)
 571 attributable to each parameter (Figure 5a), and the total variance (ST) attributable (Figure
 572 5b). We see that sensitivity is widespread, with every parameter exhibiting at a total variance
 573 attributable of >1% for at least one metric. We also see that sensitivity is overwhelmingly

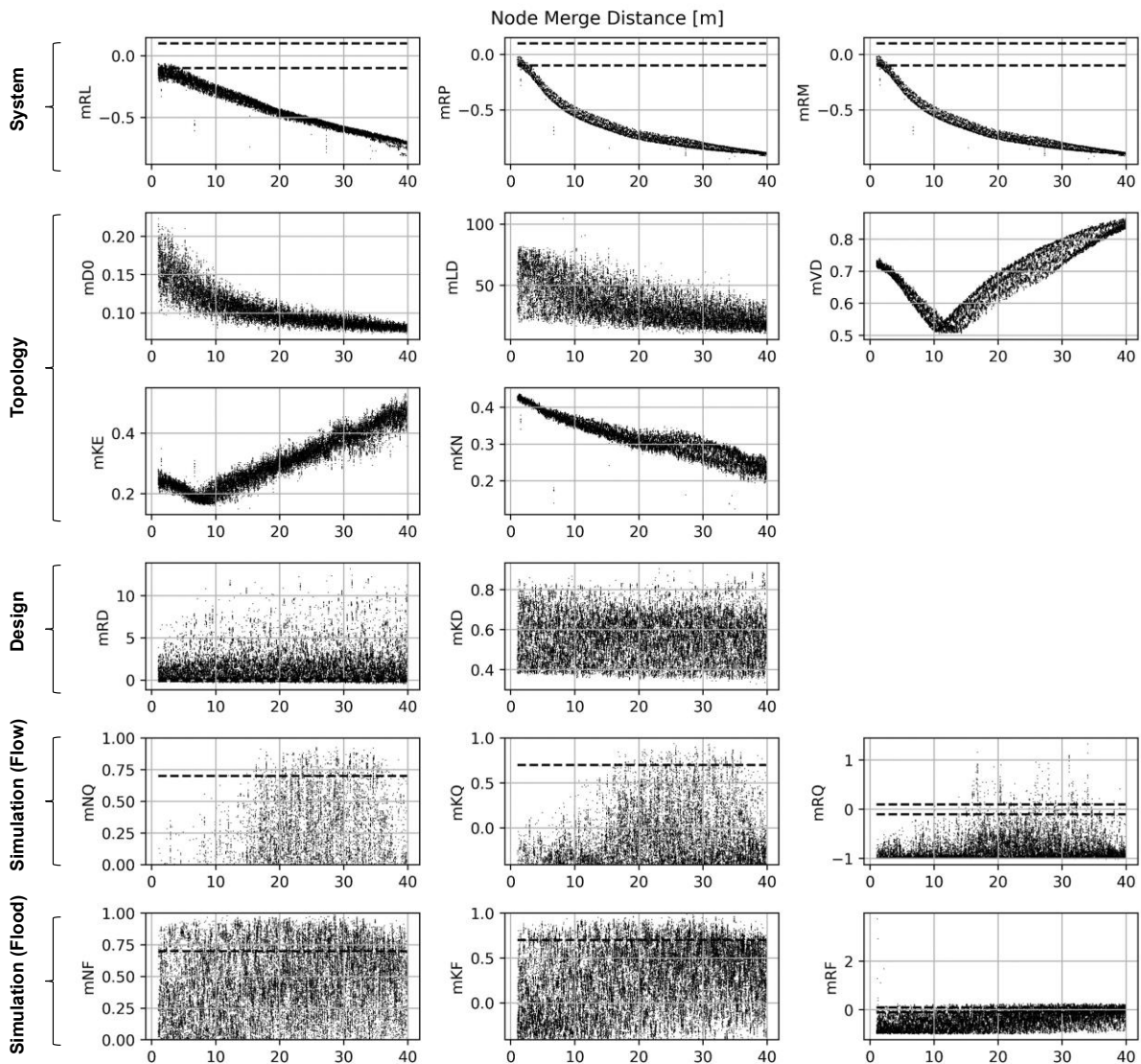
574 occurring through interactions (i.e., sensitivities present in Figure 5b but not in Figure 5a),
575 with some notable exceptions: *node merge distance* (*pNM*), *minimum velocity* (*pMV*),
576 *minimum* (*pMD*) and *maximum chamber depth* (*pXD*). First order sensitivity indicates that
577 the parameter is sensitive regardless of other parameter values, *pMV* and *pNM* are evidently
578 dominant in their influence on pipe design while *pNM* is discussed below. Second order
579 variance indices were also calculated, but not included because their confidence intervals
580 were prohibitively large.

581 Across metrics the *node merge distance* is the most sensitive parameter, impacting both
582 system description metrics (top rows), topology metrics (middle rows), and simulation
583 metrics (bottom rows). It is a sensitive parameter because it interacts with three key
584 elements in SWMManywhere:

- 585 - It influences manhole placement, which is also impacted by *max street length* (*pXS*,
586 another sensitive parameter).
- 587 - It impacts which nodes can drain to where, which is also impacted by *river buffer*
588 *distance* (*pRB*, another sensitive parameter).
- 589 - It can significantly alter how the road layout is translated into potential pipes, which
590 no other parameter does. For example, two adjacent roads running parallel may not
591 have a driving connection between them, and thus no potential pipe may span them,
592 but if these nodes are merged then a pipe could span them.

593 In addition to the dominance of these three parameters (*node merge distance*, *max street*
594 *length* and *river buffer distance*), we see many other intuitively appropriate sensitivities.
595 System metrics are sensitive to system parameters, topological metrics to topological
596 parameters, and design metrics to design parameters. We also find that flow simulation
597 metrics are sensitive to parameters relating to network topology, indicating that topology is
598 primarily influencing the global behaviour of the UDM. In contrast, we see that flood
599 simulation metrics are more sensitive to design parameters, indicating that design is
600 primarily influencing the local behaviour of the UDM.

601 We provide a specific examination of *node merge distance*, selected because it is the most
 602 sensitive parameter, to illustrate how SWMMAnywhere can be used to provide a detailed
 603 parametric exploration. We plot the parameter value of *node merge distance* against each
 604 metric value for all sampled points in Figure 6. We see clear evidence of first order sensitivity
 605 in line with those reported in Figure 5a-b.



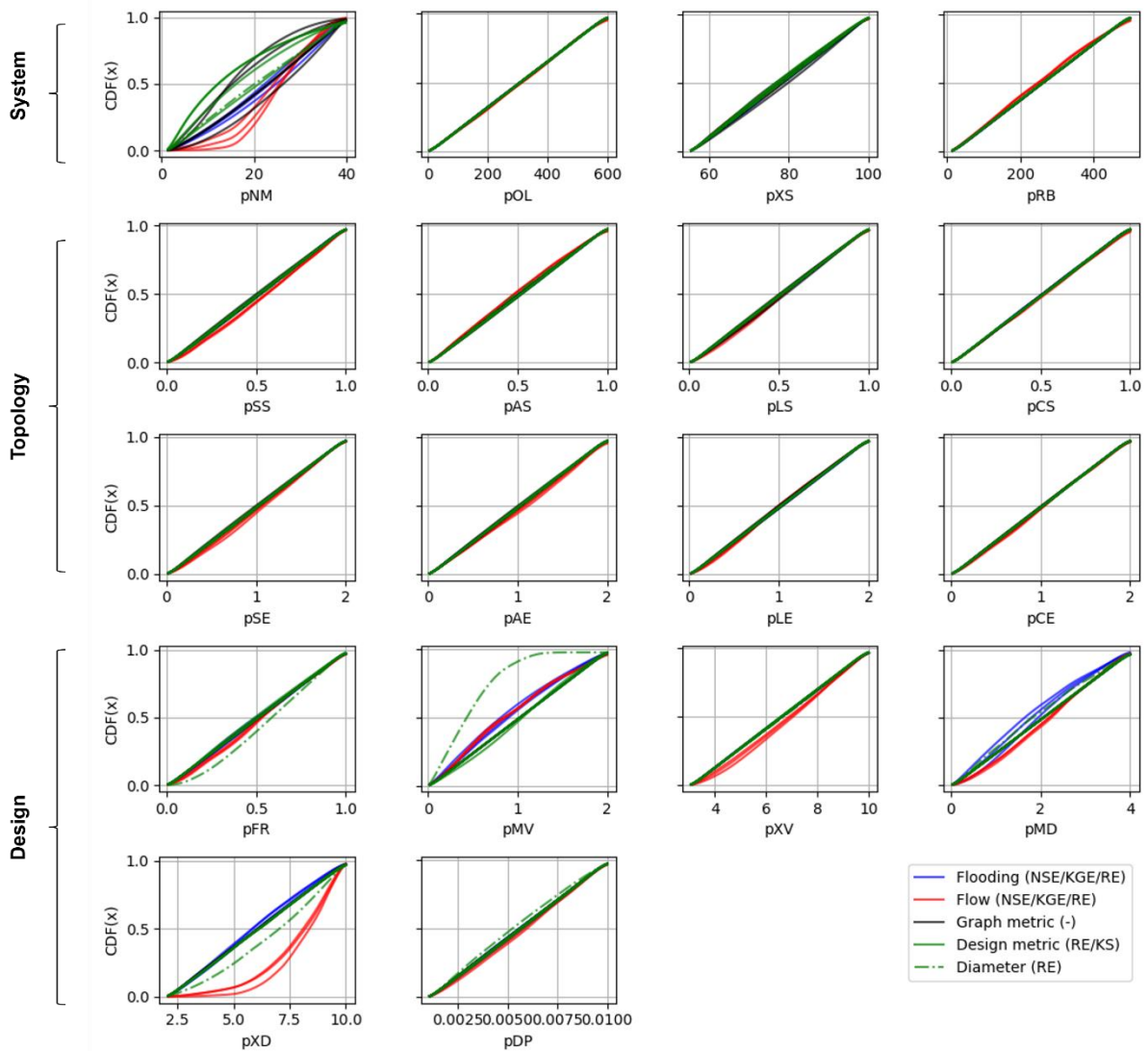
606

607 *Figure 6: Node merge distance parameter value plotted against all evaluated performance metrics. Based on*
 608 *simulations in the Cran Brook network. Panels showing NSE or KGE are clipped at 0.0 and -0.41 respectively,*
 609 *which indicates the performance of taking the mean value of observations as the simulation. Dashed lines for*
 610 *KGE, NSE, relative error indicate a region of 'behavioural' performance, that is, values >0.7 (KGE, NSE) or within*
 611 *+/- 0.1 (relative error).*

612 Figure 6 indicates some evidence of identifiable parameter values, e.g., we observe that the
 613 *node merge distance* should fall around 25m for the simulation flow metrics. However, this

614 value can vary depending on which metric is used, for example, System metrics (mRL , mRP ,
615 and mRM) and some topology metrics (mVD , mKE , mKN) indicate better performance when
616 *node merge distance* is around 0-15m.

617 It can be more informative to investigate whether parameters are identifiable using a
618 Gaussian kernel density estimate (KDE), which can be used to create a cumulative density
619 function for each parameter and can be weighted by different metrics. For example, in Figure
620 7, top left panel (pNM), weighting the KDE by flow simulations (red lines), we can see that
621 75% of the distribution indicates that *node merge distance* should be greater than 20m,
622 agreeing with Figure 6. The KDE plots further highlight identifiability for a range of other
623 parameters, however, as with *node merge distance*, in most cases there can be
624 disagreement depending on which metric is used for weighting.



625

626 *Figure 7: Gaussian KDE cumulative density functions for parameters, weighted by different metrics evaluated on*
 627 *the Cran Brook network. Metrics are grouped by colour to highlight different behaviours.*

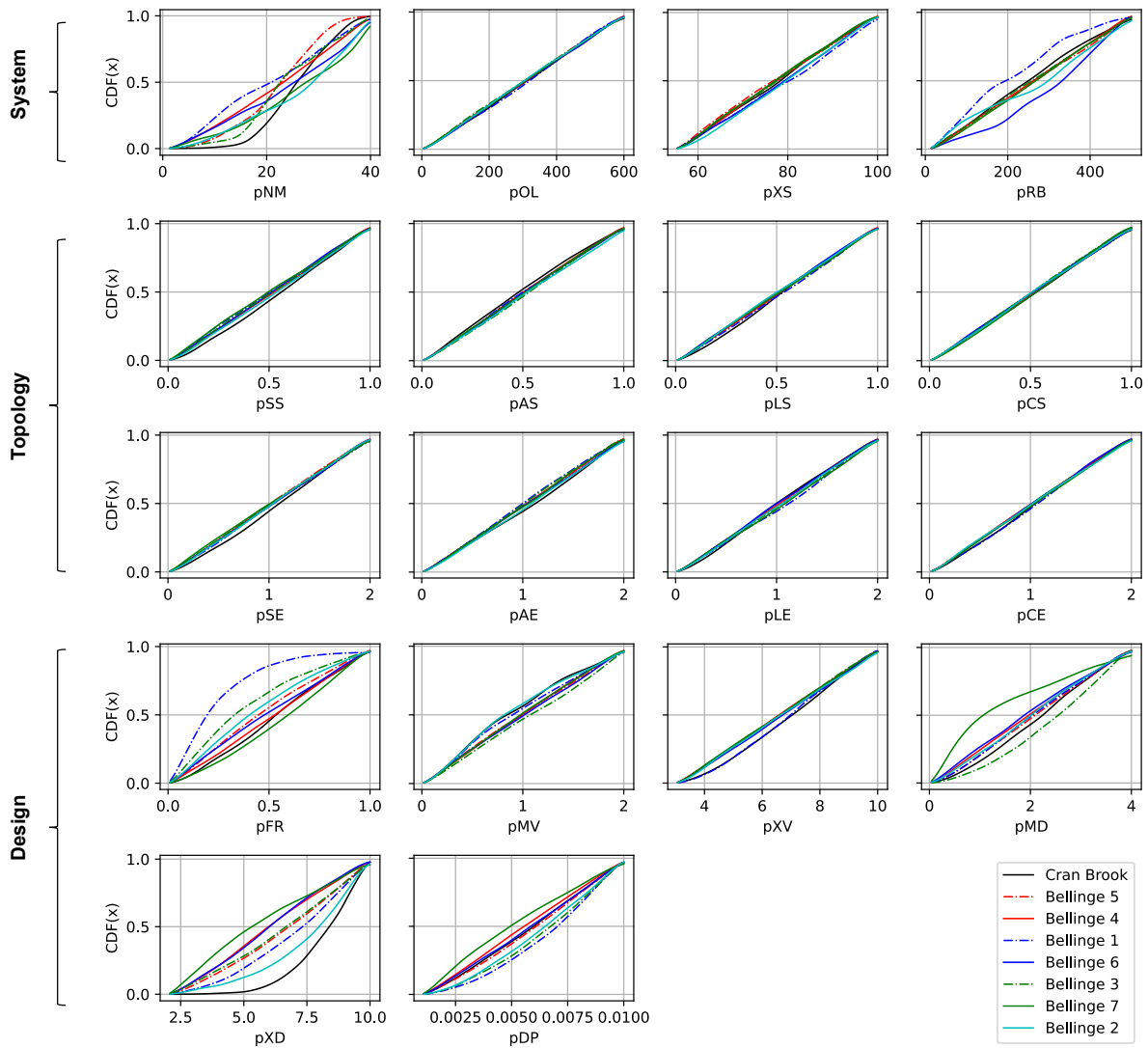
628 4.3 Sensitivity analysis, other locations

629 In Figure 5 c-f we show the sensitivity analysis results for the Bellinge 1 and 7 networks,
 630 which are the largest and smallest networks in the Bellinge dataset, respectively. Results for
 631 the other Bellinge UDMs are shown in Supplemental Figure S1, although do not
 632 meaningfully differ from the observations below.

633 In general, we see many similarities between the two analyses, including high sensitivity of
 634 *node merge distance*, more sensitivity occurring through interactions (Figure 5 c and e) than
 635 in first order (Figure 5 d and f). In contrast, we see less significance of network topology
 636 parameters across all metrics, which we can likely be attributed to smaller sizes of both

637 Bellinge networks are comparing to the Cran Brook network resulting in availability of fewer
638 topological configurations, thus less significance in terms of impacting metrics. We note that
639 no indices for flooding metrics could be calculated because the network did not experience
640 flooding under the precipitation timeseries used.

641 In Figure 8 we show the KDE estimates of parameter distributions for each network,
642 weighted by the NSE flow metric (mNQ). In contrast to Figure 7, we see stronger agreement
643 across networks than across metrics for weighting. For example, *max fr* (pXF), *precipitation*
644 (pDP), *max depth* (pXD), tend towards aligned parameter distributions across most
645 networks. Despite this, we also see some sensitive parameters with less agreement across
646 networks. For example, *min v* (pMV), *max street length* (pXS), and *node merge distance*
647 (pNM) have unaligned but identifiable parameter values. We also see that many parameters
648 do not have clearly defined distributions for most networks but do for one/few. For example,
649 *river buffer distance* appears to have a clearly defined distribution for Cran Brook and
650 Bellinge 2, while no other networks do. We do not see clear parameter distributions for
651 network topology parameters, despite their sensitivity demonstrated in Figure 5.



652

653 *Figure 8: Gaussian KDE cumulative density function for parameters for each location. Weighted by outfall flow*
 654 *NSE.*

655 **5 Discussion**

656 **5.1 Development of SWMMAnywhere**

657 In this study, we provide new insight into the intricacies of UDM synthesis through
 658 application of our proposed SWMMAnywhere workflow and performing extensive sensitivity
 659 analysis.

660 We demonstrate in Figure 4 that reasonable simulations are achievable, with NSE values of
 661 >0.7 for both outfall flow and flooding, Figure 6. The implementation based on Duque et. al.,
 662 (2022)'s pipe-by-pipe method results in high efficiency UDMs, although we observe that the

663 synthesised UDMs are perhaps too efficient as they drain the network too quickly, see flow
664 and flood simulations in Figure 4. This finding suggests that inefficiencies seen in the real
665 network reflect the additional constraints not captured by data sources that we employ in our
666 workflow, for example, incremental construction of the network (Rauch et al., 2017). Despite
667 such shortcomings, we recommend that sensitivity analysis is a necessary precursor to
668 introducing any further complexity.

669 The sensitivity analysis results, Figure 5, show widespread and intuitively sensible sensitivity
670 of all parameters, including those introduced as technical innovations of this paper: enabling
671 slope inclusion within the MSA and contributing area as a factor in the network topology
672 derivation (pSS , pCS , pSE , pCE). We also highlight the dominant sensitivity of *node merge*
673 *distance* (pNM), which influences manhole locations, outfall locations, and underlying street
674 graph preprocessing. Manhole locations are well established to be important factors
675 (Chahinian et al., 2019; Blumensaat et al., 2012), while to our knowledge this is the first
676 UDM synthesis study that treats outfall locations as an explicit unknown. The importance of
677 the underlying street graph that *node merge distance* controls is intuitively sensible, as a
678 UDM synthesis can only ever be as good as the potential pipe-carrying locations that it
679 begins with. These findings indicate a promising outlook for UDM synthesis, as manhole
680 locations, outfall locations, and the street graph are all surface elements whose estimation
681 will only improve with improved satellite imagery and machine learning. Furthermore, in
682 cases where SWMManywhere is to be applied to a local area, surveying these surface
683 elements is likely to be far less costly than a below-ground network survey.

684 5.2 Transferability of SWMManywhere

685 A key motivation for performing sensitivity analysis is in identifying behavioural parameter
686 ranges. In an ideal case, behavioural parameter ranges align across metrics and locations,
687 thus implying that parameter choices are good under any condition. Figure 7 and Figure 8
688 demonstrate that we do not see clear evidence of this for either metrics or locations
689 respectively. Figure 5 demonstrates that parameters are generally sensitive through

690 interactions, rather than through first order effects, which limits the ability to provide clear
691 advice on behavioural ranges. Although second order effects were calculated, the
692 confidence intervals were such that no conclusions could be drawn, and we estimate that
693 multiple magnitudes more samples would be required to provide definitive results, which is
694 outside the scope of this paper, but future work may investigate. Parameters that have high
695 first order sensitivity provide some clear advice, for example, *node merge distance* values
696 should be between 20m-35m to provide good flow simulation metrics in a variety of
697 locations. However, the dominant finding on parameter transferability is that the panacea of
698 arriving to a single 'correct' UDM through a synthesis approach is false. Indeed, we believe
699 that widespread findings of equifinality in hydraulic calibration of real UDMs, (Huang et al.,
700 2022; Sytsma et al., 2022) supports that the idea of having a single 'correct' UDM that is
701 based on survey information (rather than synthesis) is also false. We propose that data
702 uncertainty will remain a fundamental element of UDM, synthetic or otherwise, for the
703 foreseeable future.

704 We therefore advocate for an approach to UDM that is uncertainty driven. Rather than
705 narrowly focussing on aligning synthetic with real UDMs, a synthetic UDM may most
706 appropriately be considered one hypothesis for the underlying system. Further
707 developments to SWMManywhere should thus seek to synthesise UDMs that are plausible
708 hypotheses, possibly through a more iterative approach that refines the UDM based on
709 simulation data only, for example, by assessing SWMM continuity errors. In a no field data
710 setting, the focus could shift to, for example, various climate scenarios or future urban
711 development, to study an ensemble of plausible UDMs and explore their likely outcomes. If
712 such studies would prohibitively increase simulation time, a range of network complexity
713 reduction techniques have been demonstrated for UDMs (Farina et al., 2023; Palmitessa et
714 al., 2022), including as part of an uncertainty ensemble approach (Dobson et al., 2022;
715 Thrysøe et al., 2019).

716 To ensure that our proposed workflow is applicable at the global scale, we have deliberately
717 avoided some data, for example design regulations or a higher resolution DEM, that are
718 commonly available at national scales. In local applications, however, we do recommend
719 exploring utilising the best quality data available and adapting the underlying datasets or
720 parameter assumptions, which our SWMManywhere implementation supports. Nevertheless,
721 we caution that this may not provide the certainty that one might expect. For example, as our
722 KDE parameter estimates demonstrate in Bellinge, Denmark (Figure 8), design regulations,
723 which are parameters that are country and region specific, do not show agreement across
724 UDMs in the same locale.

725 5.3 Outlook and limitations

726 The modular graph function-based architecture of SWMManywhere makes it easy to extend
727 or customise, thus we hope that it may become a centralised location for the synthetic UDM
728 community. We see a variety of potential improvements that may be introduced to increase
729 the realism of synthesised UDMs, although we stress the importance of performing
730 sensitivity analysis before investing time in creating complicated customisations. In addition
731 to better identification of surface elements described above, other surface factors such as
732 hydraulic structures are well established to play a dominant role in UDM behaviour (Thryssøe
733 et al., 2019; Dobson et al., 2022). SWMManywhere does not attempt to synthesise these
734 structures, and they are omitted from the analysis performed in this paper. However,
735 structures such as weirs may be identifiable from satellite imagery, while including pumps
736 may form an additional element in the network topology derivation, as has been
737 demonstrated for sanitary sewer networks (Khurelbaatar et al., 2021).

738 An immediate extension to the behaviour of SWMManywhere that we are exploring is
739 around water quality. Recent literature demonstrates the feasibility of quantifying urban
740 pollution deposition on roads (Revitt et al., 2022), which could be included as an optional
741 extension, thus providing the much-needed transport element to link deposition with in-river
742 pollution. We anticipate that a key difficulty of such an approach would be in identifying

743 validation data, since sampling water quality at urban drainage outfalls during a storm is
744 dangerous to do in person. For example, while the English Environment Agency's
745 harmonised water quality sampling database contains over 60 million pollution sample
746 records since 2000 (Open water quality archive datasets (WIMS), 2024), just 0.4% are of
747 urban drainage outfalls, and only 25% of these have occurred since 2010, reflecting the
748 diminishing focus on non-compliance monitoring observed across England (Dobson et al.,
749 2021). Further improvements towards capturing water quality may also focus on
750 representing combined or misconnected systems, linking with the synthetic sanitary sewer
751 network literature (Duque et al., 2022).

752 A clear limitation of the case studies demonstrated in this paper is that they are based in
753 temperate and wealthy European countries, this is particularly problematic when considering
754 that street graph and building footprint data uncertainty will be more significant in nearly any
755 other type of region. We reached out to a variety of urban drainage modellers in both
756 industry and research but were not able to extend our case study selection further and
757 instead identified a significant paucity of publicly available reliable SWMM models. While the
758 SWMM website hosts a variety of useful example models, these aim to build understanding
759 about representing different elements of drainage networks, rather than providing a suite of
760 real test cases. Ultimately, SWMManywhere and other synthetic UDM tools will not be
761 trusted at global scales until they have been demonstrated on a wide variety of case studies.
762 Thus, we call for collaborators who can either share their SWMM models openly or are
763 willing to demonstrate SWMManywhere for their models to reach out that we may create a
764 more robust demonstration of UDM synthesis and verify that understandings created are
765 sustainable.

766 **6 Conclusion**

767 In this paper we present a workflow, SWMManywhere, that can synthesise an urban
768 drainage network model (UDM) and simulate it in SWMM, anywhere globally. We test the

769 parameters of SWMMAnywhere using sensitivity analysis to understand the dominant
770 processes involved in synthesising UDMs. Our results revealed three key findings:

- 771 1. The SWMMAnywhere workflow can synthesize high quality UDM at a range of spatial
772 scales. The parameters that can be used to tune SWMMAnywhere behave in
773 intuitively sensible ways, verifying its implementation.
- 774 2. We find that parameters controlling surface elements such as manhole locations,
775 street layout, and network outfalls are the most sensitive, and thus should be the key
776 focus of uncertainty reduction. Encouragingly, the identification of these elements is
777 also the most likely to improve in the foreseeable future.
- 778 3. UDM synthesis is sensitive to all parameters and these parameters primarily
779 influence outputs through second order or higher interactions, revealing UDM
780 synthesis to be a more complex process than previously recognised. Additionally, we
781 recommend that an ensemble approach would be appropriate for practical
782 applications to more appropriately reflect the inherent uncertainty of the underlying
783 system.

784 We hope that the urban drainage community will use SWMMAnywhere to further explore the
785 complexity of UDM synthesis, develop robust interventions in areas without existing UDM
786 data, and do so in a more open and reproducible scientific environment.

787 **7 Acknowledgements**

788 BD, TJ, DA, TC were involved in theoretical formulation of the SWMMAnywhere
789 methodology. BD, DA, TC were involved in software development, with further support
790 provided by Imperial College's Research Software Engineering service. BD, TJ, TC were
791 involved in the experimental formulation and sensitivity analysis. BD, TJ, TC, DA were
792 involved in drafting and editing the manuscript. We are also grateful to Ana Mijic for their
793 insightful comments on the manuscript that have improved the paper.

794 BD is funded through the Imperial College Research Fellowship scheme, which also funded
795 the software development. TJ time was supported by the UK Natural Environment Research
796 Council-funded CAMELLIA project (grant no. NE/S003495/1). TJ publishes with the
797 permission of the Executive Director of the British Geological Survey. We acknowledge
798 computational resources and support provided by the Imperial College Research Computing
799 Service (<http://doi.org/10.14469/hpc/2232>).

800 **8 Data availability statement**

801 The software implementation of SWMManywhere is an open-source repository available at
802 <https://github.com/ImperialCollegeLondon/SWMManywhere> (last accessed 2024-10-11). The
803 documentation for SWMManywhere can be found at
804 <https://imperialcollegelondon.github.io/SWMManywhere/> (last accessed 2024-10-11). The
805 results of the paper's experiments and code to perform sensitivity analysis and plots is
806 available at https://github.com/barneydobson/swmmanywhere_paper (last accessed 2024-
807 10-11).

808 **9 References**

- 809 Arrighi, C. and Campo, L.: Effects of digital terrain model uncertainties on high-resolution
810 urban flood damage assessment, *J. Flood Risk Manag.*, 12,
811 <https://doi.org/10.1111/jfr3.12530>, 2019.
- 812 Babovic, F. and Mijic, A.: The development of adaptation pathways for the long-term
813 planning of urban drainage systems, *J. Flood Risk Manag.*, 12,
814 <https://doi.org/10.1111/jfr3.12538>, 2019.
- 815 Bach, P. M., Rauch, W., Mikkelsen, P. S., McCarthy, D. T., and Deletic, A.: A critical review
816 of integrated urban water modelling - Urban drainage and beyond, *Environ. Model. Softw.*,
817 54, 88–107, <https://doi.org/10.1016/j.envsoft.2013.12.018>, 2014.
- 818 Bach, P. M., Kuller, M., McCarthy, D. T., and Deletic, A.: A spatial planning-support system
819 for generating decentralised urban stormwater management schemes, *Sci. Total Environ.*,
820 726, 138282, <https://doi.org/10.1016/j.scitotenv.2020.138282>, 2020.
- 821 Bertsch, R., Glenis, V., and Kilsby, C.: Urban flood simulation using synthetic storm drain
822 networks, *Water (Switzerland)*, 9, <https://doi.org/10.3390/w9120925>, 2017.
- 823 Blumensaat, F., Wolfram, M., and Krebs, P.: Sewer model development under minimum
824 data requirements, *Environ. Earth Sci.*, 65, 1427–1437, <https://doi.org/10.1007/s12665-011-1146-1>, 2012.
- 826 Boeing, G.: OSMnx: New methods for acquiring, constructing, analyzing, and visualizing
827 complex street networks, *Comput. Environ. Urban Syst.*, 65, 126–139,

- 828 <https://doi.org/10.1016/j.compenvurbsys.2017.05.004>, 2017.
- 829 Butler, D. and Davies, J. w.: Urban Drainage 2nd Edition, 566 pp., 2004.
- 830 Chahinian, N., Delenne, C., Commandré, B., Derras, M., Deruelle, L., and Bailly, J. S.:
831 Automatic mapping of urban wastewater networks based on manhole cover locations,
832 Comput. Environ. Urban Syst., 78, 101370,
833 <https://doi.org/10.1016/j.compenvurbsys.2019.101370>, 2019.
- 834 Chegini, T. and Li, H. Y.: An algorithm for deriving the topology of belowground urban
835 stormwater networks, Hydrol. Earth Syst. Sci., 26, 4279–4300, [https://doi.org/10.5194/hess-](https://doi.org/10.5194/hess-26-4279-2022)
836 [26-4279-2022](https://doi.org/10.5194/hess-26-4279-2022), 2022.
- 837 Coxon, G., McMillan, H., Bloomfield, J. P., Bolotin, L., Dean, J. F., Kelleher, C., Slater, L.,
838 and Zheng, Y.: Wastewater discharges and urban land cover dominate urban hydrology
839 signals across England and Wales, Environ. Res. Lett., 19, 084016,
840 <https://doi.org/10.1088/1748-9326/ad5bf2>, 2024.
- 841 Crippen, R., Buckley, S., Agram, P., Belz, E., Gurrola, E., Hensley, S., Kobrick, M., Lavallo,
842 M., Martin, J., Neumann, M., Nguyen, Q., Rosen, P., Shimada, J., Simard, M., and Tung, W.:
843 NASADEM GLOBAL ELEVATION MODEL: METHODS AND PROGRESS, Int. Arch.
844 Photogramm. Remote Sens. Spat. Inf. Sci., XLI-B4, 125–128, [https://doi.org/10.5194/isprs-](https://doi.org/10.5194/isprs-archives-XLI-B4-125-2016)
845 [archives-XLI-B4-125-2016](https://doi.org/10.5194/isprs-archives-XLI-B4-125-2016), 2016.
- 846 Deletic, A., Dotto, C. B. S., McCarthy, D. T., Kleidorfer, M., Freni, G., Mannina, G., Uhl, M.,
847 Henrichs, M., Fletcher, T. D., Rauch, W., Bertrand-Krajewski, J. L., and Tait, S.: Assessing
848 uncertainties in urban drainage models, Phys. Chem. Earth, 42–44, 3–10,
849 <https://doi.org/10.1016/j.pce.2011.04.007>, 2012.
- 850 Dobson, B., Jovanovic, T., Chen, Y., Paschalis, A., Butler, A., and Mijic, A.: Integrated
851 modelling to support analysis of COVID-19 impacts on London’s water system and in-river
852 water quality, Front. Water, 3, 26, <https://doi.org/10.3389/frwa.2021.641462>, 2021.
- 853 Dobson, B., Watson-Hill, H., Muhandes, S., Borup, M., and Mijic, A.: A Reduced Complexity
854 Model With Graph Partitioning for Rapid Hydraulic Assessment of Sewer Networks, Water
855 Resour. Res., 58, <https://doi.org/10.1029/2021WR030778>, 2022.
- 856 Dobson, B., Alonso-Álvarez, D., and Chegini, T.: SWMManywhere,
857 <https://doi.org/10.5281/zenodo.13837741>, September 2024a.
- 858 SWMMAnywhere documentation: <https://imperialcollegelondon.github.io/SWMMAnywhere/>,
859 last access: 4 October 2024.
- 860 Dobson, B., Alonso-Álvarez, D., and Chegini, T.: SWMMAnywhere sensitivity analysis,
861 <https://doi.org/10.5281/zenodo.13918627>, September 2024b.
- 862 Duque, N., Bach, P. M., Scholten, L., Fappiano, F., and Maurer, M.: A Simplified Sanitary
863 Sewer System Generator for Exploratory Modelling at City-Scale, Water Res., 209, 117903,
864 <https://doi.org/10.1016/j.watres.2021.117903>, 2022.
- 865 Eilander, D.: pyFlwDir: Fast methods to work with hydro-and topography data in pure python,
866 Zenodo [code], 10, 2022.
- 867 Open water quality archive datasets (WIMS): [https://environment.data.gov.uk/water-](https://environment.data.gov.uk/water-quality/view/download)
868 [quality/view/download](https://environment.data.gov.uk/water-quality/view/download), last access: 21 August 2024.
- 869 Farina, A., Di Nardo, A., Gargano, R., van der Werf, J. A., and Greco, R.: A simplified
870 approach for the hydrological simulation of urban drainage systems with SWMM, J. Hydrol.,
871 623, 129757, <https://doi.org/10.1016/j.jhydrol.2023.129757>, 2023.
- 872 Ghosh, I., Hellweger, F. L., and Fritch, T. G.: Fractal generation of artificial sewer networks

873 for hydrologic simulations, Proc. 2006 ESRI Int. User Conf., 1–12, 2006.

874 Gironás, J., Niemann, J. D., Roesner, L. A., Rodriguez, F., and Andrieu, H.: Evaluation of
875 Methods for Representing Urban Terrain in Storm-Water Modeling, *J. Hydrol. Eng.*, 15, 1–
876 14, [https://doi.org/10.1061/\(ASCE\)HE.1943-5584.0000142](https://doi.org/10.1061/(ASCE)HE.1943-5584.0000142), 2010.

877 Hagberg, A. A., Schult, D. A., and Swart, P. J.: Exploring Network Structure, Dynamics, and
878 Function using NetworkX, in: Proceedings of the 7th Python in Science Conference, 11–15,
879 2008.

880 Herman, J. and Usher, W.: SALib: An open-source Python library for Sensitivity Analysis, *J.*
881 *Open Source Softw.*, 2, 97, <https://doi.org/10.21105/joss.00097>, 2017.

882 Huang, Y., Zhang, J., Zheng, F., Jia, Y., Kapelan, Z., and Savic, D.: Exploring the
883 Performance of Ensemble Smoothers to Calibrate Urban Drainage Models, *Water Resour.*
884 *Res.*, 58, 1–22, <https://doi.org/10.1029/2022WR032440>, 2022.

885 Hutton, C., Wagener, T., Freer, J., Han, D., Duffy, C., and Arheimer, B.: Most computational
886 hydrology is not reproducible, so is it really science?, *Water Resour. Res.*, 52, 7548–7555,
887 <https://doi.org/10.1002/2016WR019285>, 2016.

888 Subcatchment Data Fields (InfoWorks):
889 [https://help2.innovyze.com/infoworksicm/Content/HTML/ICM_IL/Subcatchment_Data_Fields.](https://help2.innovyze.com/infoworksicm/Content/HTML/ICM_IL/Subcatchment_Data_Fields.htm)
890 [htm](https://help2.innovyze.com/infoworksicm/Content/HTML/ICM_IL/Subcatchment_Data_Fields.htm), last access: 3 June 2024.

891 Khurelbaatar, G., Al Marzuqi, B., Van Afferden, M., Müller, R. A., and Friesen, J.: Data
892 Reduced Method for Cost Comparison of Wastewater Management Scenarios–Case Study
893 for Two Settlements in Jordan and Oman, *Front. Environ. Sci.*, 9,
894 <https://doi.org/10.3389/fenvs.2021.626634>, 2021.

895 Li, X. and Willems, P.: A hybrid model for fast and probabilistic urban pluvial flood prediction,
896 *Water Resour. Res.*, 1–26, <https://doi.org/10.1029/2019wr025128>, 2020.

897 Lindsay, J. B.: Efficient hybrid breaching-filling sink removal methods for flow path
898 enforcement in digital elevation models, *Hydrol. Process.*, 30, 846–857,
899 <https://doi.org/10.1002/hyp.10648>, 2016a.

900 Lindsay, J. B.: Whitebox GAT: A case study in geomorphometric analysis., *Comput. Geosci.*,
901 95, 75–84, 2016b.

902 Mair, M., Zischg, J., Rauch, W., and Sitzenfrie, R.: Where to find water pipes and sewers?–
903 On the correlation of infrastructure networks in the urban environment, *Water (Switzerland)*,
904 9, <https://doi.org/10.3390/w9020146>, 2017.

905 McDonnell, B., Ratliff, K., Tryby, M., Wu, J., and Mullapudi, A.: PySWMM: The Python
906 Interface to Stormwater Management Model (SWMM), *J. Open Source Softw.*, 5, 2292,
907 <https://doi.org/10.21105/joss.02292>, 2020.

908 Computer generated building footprints for the United States:
909 <https://github.com/Microsoft/USBuildingFootprints?tab=readme-ov-file>, last access: 30 July
910 2024.

911 Möderl, M., Butler, D., and Rauch, W.: A stochastic approach for automatic generation of
912 urban drainage systems, *Water Sci. Technol.*, 59, 1137–1143,
913 <https://doi.org/10.2166/wst.2009.097>, 2009.

914 Möderl, M., Sitzenfrie, R., Fetz, T., Fleischhacker, E., and Rauch, W.: Systematic generation
915 of virtual networks for water supply, *Water Resour. Res.*, 47, 1–10,
916 <https://doi.org/10.1029/2009WR008951>, 2011.

917 Montalvo, C., Reyes-Silva, J. D., Sañudo, E., Cea, L., and Puertas, J.: Urban pluvial flood

- 918 modelling in the absence of sewer drainage network data: A physics-based approach, J.
919 Hydrol., 634, 131043, <https://doi.org/10.1016/j.jhydrol.2024.131043>, 2024.
- 920 O'Callaghan, J. F. and Mark, D. M.: The extraction of drainage networks from digital
921 elevation data, *Comput. Vision, Graph. Image Process.*, 28, 323–344,
922 [https://doi.org/10.1016/S0734-189X\(84\)80011-0](https://doi.org/10.1016/S0734-189X(84)80011-0), 1984.
- 923 Ochoa-Rodriguez, S., Wang, L. P., Gires, A., Pina, R. D., Reinoso-Rondinel, R., Bruni, G.,
924 Ichiba, A., Gaitan, S., Cristiano, E., Van Assel, J., Kroll, S., Murlà-Tuyls, D., Tisserand, B.,
925 Schertzer, D., Tchiguirinskaia, I., Onof, C., Willems, P., and Ten Veldhuis, M. C.: Impact of
926 spatial and temporal resolution of rainfall inputs on urban hydrodynamic modelling outputs: A
927 multi-catchment investigation, *J. Hydrol.*, 531, 389–407,
928 <https://doi.org/10.1016/j.jhydrol.2015.05.035>, 2015.
- 929 Palmitessa, R., Grum, M., Engsig-Karup, A. P., and Löwe, R.: Accelerating hydrodynamic
930 simulations of urban drainage systems with physics-guided machine learning, *Water Res.*,
931 223, 118972, 2022.
- 932 Pedersen, A., Pedersen, J., Viguera-Rodriguez, A., Brink-Kjær, A., Borup, M., and
933 Mikkelsen, P.: The Bellinge data set: open data and models for community-wide urban
934 drainage systems research, *Earth Syst. Sci. Data Discuss.*, 13, 4779–4798,
935 <https://doi.org/10.5194/essd-2021-8>, 2021.
- 936 Pianosi, F., Beven, K., Freer, J., Hall, J. W., Rougier, J., Stephenson, D. B., and Wagener,
937 T.: Sensitivity analysis of environmental models: A systematic review with practical workflow,
938 *Environ. Model. Softw.*, 79, 214–232, <https://doi.org/10.1016/j.envsoft.2016.02.008>, 2016.
- 939 Rauch, W., Urich, C., Bach, P. M., Rogers, B. C., de Haan, F. J., Brown, R. R., Mair, M.,
940 McCarthy, D. T., Kleidorfer, M., Sitzenfrei, R., and Deletic, A.: Modelling transitions in urban
941 water systems, *Water Res.*, 126, 501–514, <https://doi.org/10.1016/j.watres.2017.09.039>,
942 2017.
- 943 Ray, G. and Sen, A.: Minimal spanning arborescence, *arXiv Prepr. arXiv2401.13238*, 2024.
- 944 Revitt, D. M., Ellis, J. B., Gilbert, N., Bryden, J., and Lundy, L.: Development and application
945 of an innovative approach to predicting pollutant concentrations in highway runoff, *Sci. Total*
946 *Environ.*, 825, 153815, 2022.
- 947 Reyes-Silva, J. D., Novoa, D., Helm, B., and Krebs, P.: An Evaluation Framework for Urban
948 Pluvial Flooding Based on Open-Access Data, *Water (Switzerland)*, 15,
949 <https://doi.org/10.3390/w15010046>, 2023.
- 950 Rossman, L. A.: Storm water management model user's manual, version 5.0, Cincinnati, 72–
951 73 pp., 2010.
- 952 Saltelli, A., Ratto, M., Andres, T., Campolongo, F., Cariboni, J., Gatelli, D., Saisana, M., and
953 Tarantola, S.: *Global Sensitivity Analysis. The Primer*, Wiley, John & Sons, 1–292 pp.,
954 <https://doi.org/10.1002/9780470725184>, 2008.
- 955 Saltelli, A., Aleksankina, K., Becker, W., Fennell, P., Ferretti, F., Holst, N., Li, S., and Wu, Q.:
956 Why so many published sensitivity analyses are false: A systematic review of sensitivity
957 analysis practices, *Environ. Model. Softw.*, 114, 29–39,
958 <https://doi.org/10.1016/j.envsoft.2019.01.012>, 2019.
- 959 Seo, Y. and Schmidt, A. R.: Network configuration and hydrograph sensitivity to storm
960 kinematics, *Water Resour. Res.*, 49, 1812–1827, <https://doi.org/10.1002/wrcr.20115>, 2013.
- 961 Sirko, W., Kashubin, S., Ritter, M., Annkah, A., Bouchareb, Y. S. E., Dauphin, Y. N.,
962 Keyzers, D., Neumann, M., Cissé, M., and Quinn, J.: Continental-Scale Building Detection
963 from High Resolution Satellite Imagery, *CoRR*, abs/2107.1, 2021.

- 964 Sobol, I. M.: Sensitivity estimates for nonlinear mathematical models, *Math. Model. Comput. Exp.*, 1, 407, 1993.
965
- 966 Source, M. O., McFarland, M., Emanuele, R., Morris, D., and Augspurger, T.:
967 microsoft/PlanetaryComputer: October 2022, <https://doi.org/10.5281/zenodo.7261897>,
968 October 2022.
- 969 Stagge, J. H., Rosenberg, D. E., Abdallah, A. M., Akbar, H., Attallah, N. A., and James, R.:
970 Assessing data availability and research reproducibility in hydrology and water resources,
971 *Sci. Data*, 6, 190030, <https://doi.org/10.1038/sdata.2019.30>, 2019.
- 972 Sun, S., Djordjevic, S., and Khu, S. T.: A general framework for flood risk-based storm sewer
973 network design, *Urban Water J.*, 8, 13–27, <https://doi.org/10.1080/1573062X.2010.542819>,
974 2011.
- 975 Sweetapple, C., Fu, G., Farmani, R., Meng, F., Ward, S., and Butler, D.: Attribute-based
976 intervention development for increasing resilience of urban drainage systems, *Water Sci.*
977 *Technol.*, 77, 1757–1764, <https://doi.org/10.2166/wst.2018.070>, 2018.
- 978 Sytsma, A., Crompton, O., Panos, C., Thompson, S., and Mathias Kondolf, G.: Quantifying
979 the Uncertainty Created by Non-Transferable Model Calibrations Across Climate and Land
980 Cover Scenarios: A Case Study With SWMM, *Water Resour. Res.*, 58, 1–21,
981 <https://doi.org/10.1029/2021WR031603>, 2022.
- 982 Tan, M. and Le, Q. V: EfficientNet: Rethinking Model Scaling for Convolutional Neural
983 Networks, *CoRR*, abs/1905.1, 2019.
- 984 Tarjan, R. E.: Finding optimum branchings, *Networks*, 7, 25–35,
985 <https://doi.org/10.1002/net.3230070103>, 1977.
- 986 Thrysoe, C., Arnbjerg-Nielsen, K., and Borup, M.: Identifying fit-for-purpose lumped
987 surrogate models for large urban drainage systems using GLUE, *J. Hydrol.*, 568, 517–533,
988 <https://doi.org/10.1016/j.jhydrol.2018.11.005>, 2019.
- 989 Google-Microsoft Open Buildings: [https://beta.source.coop/repositories/vida/google-](https://beta.source.coop/repositories/vida/google-microsoft-open-buildings)
990 [microsoft-open-buildings](https://beta.source.coop/repositories/vida/google-microsoft-open-buildings), last access: 30 July 2024.
- 991 Warsta, L., Niemi, T. J., Taka, M., Krebs, G., Haahti, K., Koivusalo, H., and Kokkonen, T.:
992 Development and application of an automated subcatchment generator for SWMM using
993 open data, *Urban Water J.*, 14, 954–963, <https://doi.org/10.1080/1573062X.2017.1325496>,
994 2017.
- 995 Wills, P. and Meyer, F. G.: Metrics for graph comparison: A practitioner’s guide, *PLoS One*,
996 15, e0228728, <https://doi.org/10.1371/journal.pone.0228728>, 2020.
- 997 Xu, Z., Dong, X., Zhao, Y., and Du, P.: Enhancing resilience of urban stormwater systems:
998 cost-effectiveness analysis of structural characteristics, *Urban Water J.*, 18, 850–859,
999 <https://doi.org/10.1080/1573062X.2021.1941139>, 2021.

1000